[19] a) R. L. Woodin, J. L. Beauchamp, *J. Am. Chem. Soc.* **1978**, *100*, 501; b) B. C. Guo, J. W. Purnell, A. W. Castelman, *Chem. Phys. Lett.* **1990**, *168*, 155; c) J. Sunder, K. Nishizawa, P. Kebarle, *J. Phys. Chem.* **1981**, *85*, 1814; d) M. Tacke, *Eur. J. Inorg. Chem.* **1998**, 537.

[20] Recent calculations on related species such as $[R_2MMR_2]^{2-}$ (M = Al, Ga, In, Tl) indicate strong solvation of the countercation is the key to their stabilization. A. J. Bridgeman, N. A. Nielsen, *Inorg. Chim. Acta* **2000**, *303*, 107.

Light-Driven Microfabrication: Assembly of Multicomponent, Three-Dimensional Structures by Using Optical Tweezers**

R. Erik Holmlin, Michele Schiavoni, Clifford Y. Chen, Stephen P. Smith, Mara G. Prentiss, and George M. Whitesides*

Methods to generate well-defined structures composed of cells have the potential to be useful in areas where aggregates of cells are relevant: a) analytical systems that use cells as sensors; b) systems for fundamental studies of metabolism, signaling, toxicology, cellular ecology, and the biophysics of cell–cell interactions; and c) systems that investigate relationships between cell attachment, development, and growth. Here, we have used optical tweezers to fabricate ordered, two-dimensional (2D) and three-dimensional (3D), composite microstructures in which the components are biological cells (erythrocytes and lymphocytes) and polystyrene microspheres. This method of fabrication, light-driven microfabrication, provides a method of generating a range of structurally well-defined arrays of cells in the form of composites incorporating cells and microspheres.

Figure 1 illustrates the important elements of light-driven microfabrication. We used erythrocytes, disk-shaped cells approximately 12 μm in width, and lymphocytes, roughly spherical cells approximately 5 μm in diameter, as model components with which to explore microassembly. The surfaces of these cells present multiple oligosaccharides that terminate in *N*-acetyl glucosamine (GlcNAc) and *N*-acetyl neuraminic acid (NeuAc);[1] these sugars provide well-defined ligands when biospecific adhesion is required. There are three potential mechanisms for the attachment of cells to surfaces: nonbiospecific interactions (e.g. hydrogen bonds,[2] hydrophobic interactions,[2] or electrostatic interactions);[3] biospecific interactions that are exclusively adhesive (for example, lectins binding to sugars);[4] and biospecific interactions that are both adhesive and functional (for example, integrins binding to RGD (peptide sequence Arg–Gly–Asp) or fibronectin;[5] selectins binding to cadherins).[6] To connect cells biospecifically, we used polystyrene microspheres linked covalently to wheat germ agglutinin (WGA), a well-characterized dimeric lectin that recognizes NeuAc and GlcNAc;[7, 8] to connect cells nonbiospecifically, we used unmodified polystyrene microspheres. It should also be possible to use

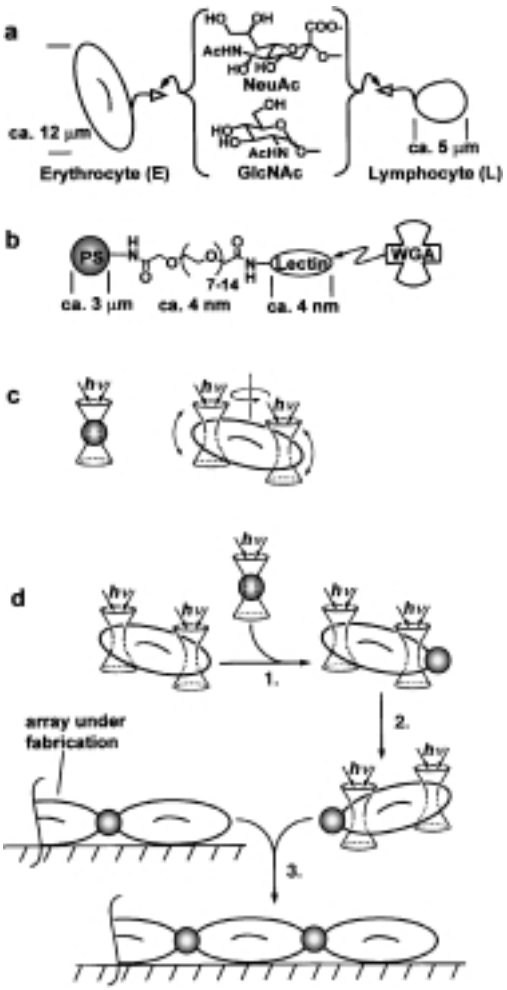

Figure 1. Fabrication of composite structures of cells and polymer microspheres by using optical tweezers. a) The oligosaccharides on surfaces of a chicken erythrocyte and chicken lymphocyte terminate in *N*-acetyl neuraminic acid (NeuAc) and *N*-acetyl glucosamine (GlcNAc). b) A polystyrene microsphere (3 μm in diameter) is linked with WGA, a lectin that binds to NeuAc and GlcNAc. c) One optical trap is used to support a WGA-linked microsphere, and two optical trapping beams orient and transport an erythrocyte. d) Light-driven microfabrication has three steps: The sequence begins with a cell supported in two traps. 1.) We use a third trap to bring a microsphere into contact with the surface of the cell. The sphere adheres to the cell by polyvalent, biospecific interactions between WGA and the NeuAc and GlcNAc groups. 2.) The two traps focused on the erythrocyte (with the attached microsphere) move the aggregate of microsphere and cell into the orientation desired for further steps in fabrication. 3.) The multiple traps are translated to bring the microsphere that is attached to the cell into contact with an assembly that is resting on the glass floor of the sample container. Repetition of this procedure generates the desired structure.

[*] Prof. G. M. Whitesides, Dr. R. E. Holmlin
Department of Chemistry and Chemical Biology
Harvard University, 12 Oxford Street
Cambridge, MA 02138 (USA)
Fax: (+1) 617-495-9857
E-mail: gwhitesides@gmwgroup.harvard.edu
M. Schiavoni, C. Y. Chen, S. P. Smith, Prof. M. G. Prentiss
Department of Physics, Harvard University
17 Oxford Street, Cambridge, MA 02138 (USA)

[**] This work was supported by DARPA (G.M.W.), the NIH (G.M.W.), and MRSEC (G.M.W., M.G.P.). R.E.H. thanks the NIH for a postdoctoral fellowship. We thank Emanuele Ostuni and Dr. Shuichi Takayama for helpful discussions.

  1433-7851/00/3919-3503 $ 17.50+.50/0

functional biospecific interactions between cell-adhesion molecules on the surface of microspheres and receptors on the surface of mammalian cells; we believe that this mode of attachment will provide a way to examine the influence of cell-surface interactions within structured aggregates of anchorage-dependent cells.[9]

The essential feature of light-driven microfabrication is the application of optical tweezers, focused beams of light that can be used to hold, orient, and move transparent objects that have a refractive index greater than that of the surrounding medium.[10] These optical tweezers are used to bring cells and microspheres into contact,[11] and to control the geometry of the resulting assemblies (Figure 1c). We used a single beam to support the polystyrene microsphere. By training two beams on different parts of the erythrocyte, we are able to control both its position and orientation. Lymphocytes are roughly spherical, and settle into the focal region of a single laser beam. Figure 1d outlines the procedure for light-driven microfabrication.

Figure 2 shows several 2D structures. In each of these images, the structures rest on the surface of the glass microscope slide immersed in buffer. The erythrocytes are lying on the surface with their flat face facing into the line of sight. The different shadings of the polystyrene microspheres reflect the fact that they lie in slightly different positions relative to the focal planes in each structure; the brighter the sphere, the closer it is to the focal plane of the camera.

In structures 2a–2c and 2e, the cells are connected by biospecific interactions between WGA on the surface of the microspheres and NeuAc or GlcNAc on the surface of the erythrocytes. On basis of five observations we inferred that this adhesion was biospecific: a) upon contact, the WGA-linked microspheres adhered to the surface of the erythrocytes and could not be detached with optical forces over the range of 0.1–10 pN. b) Soluble carbohydrates that bind to WGA inhibited the adhesion: 15 mM GlcNAc, 0.05 mM *N*,*N*′-diacetylchitobiose ($GlcNAc_2$), or 0.01 mM tetra-*N*-acetylchitotetraose ($GlcNAc_4$) reduced the probability of adhesion (P^{ADH}) between the sphere and the cell to approximately 0.5 (P^{ADH} is the ratio of the number of times a sphere adhered to the surface of a cell to the total number of collisions between cell and sphere); increasing the concentration of the inhibitor by a factor of approximately 10 blocked the adhesion completely ($P^{ADH} = 0$). c) Glucose (200 mM), which does not bind to WGA,[7, 8] had no detectable effect on the adhesion. d) Microspheres to which oligomers of ethylene glycol were attached instead of WGA did not adhere to the cells.[11] e) Individual WGA-linked microspheres did not adhere to each other.

Although the interactions between the individual binding sites of WGA and carbohydrates are relatively weak (dissociation constant $K_d^{GlcNAc} = 5$ mM;[4] $K_d^{NeuAc} = 2$ mM[12]), the spheres adhered strongly to the erythrocytes. We believe the strength of this adhesion reflects polyvalency[13] in the interactions between multiple WGA molecules on the surface of the microsphere and multiple copies of sugar groups on the cell surface. The observation that these polyvalent interactions can be antagonized biospecifically at values of concentrations of sugars close to their values of K_d for WGA is also compatible with polyvalency being the source of the strong binding between the microspheres and the cells.[14, 15] Polyvalency makes it possible to use relatively weak interactions to design biospecific interactions to connect micron-scaled objects; a precondition is that the surface densities of receptors and ligands are sufficiently large.

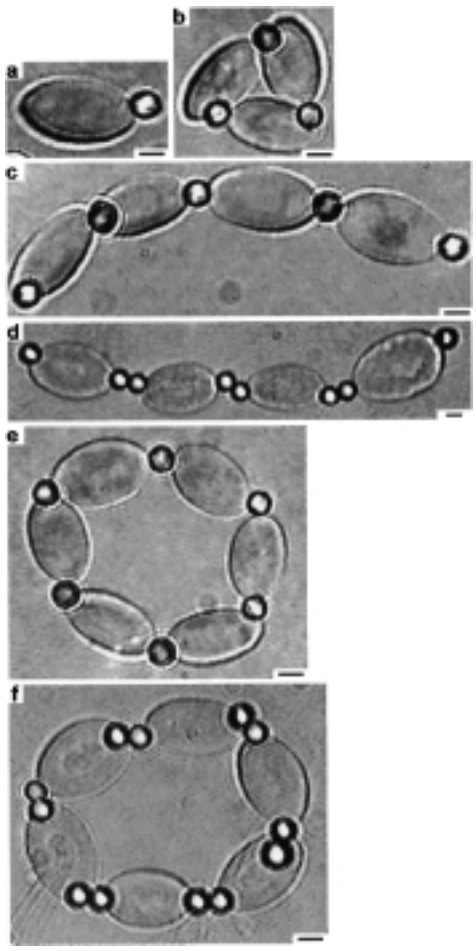

Figure 2. Optical micrographs of 2D microstructures fabricated by light-driven microfabrication. The structures in a)–c) and e) are connected by biospecific interactions between lectin-coated microspheres and sugars on the cell surfaces; structures d) and f) are connected by nonbiospecific interactions in which bare polystyrene microspheres adhere both to the cells and to one another. a) One microsphere coated with WGA attached to the surface of a single erythrocyte. b) Triangular network of three erythrocytes connected by three microspheres. c) Linear array of four erythrocytes with three bridging microspheres and two terminal microspheres. d) Linear array of four erythrocytes connected by nonbiospecific interactions. e) Hexagonal microstructure of six erythrocytes and six microspheres. f) Hexagonal structure of six erythrocytes joined by nonbiospecific interactions. We refer to these arrays as 2D because that is an approximate description of their shape, they do not, however, have an essential characteristic of 2D assemblies: that is, that one or more nodes connect to three (rather than two) other nodes. The bar in each image represents 3 μm.

By using reversible biospecific interactions to connect the cells and microspheres enables these structures to be disassembled biospecifically. After generating 2D arrays of erythrocytes, we introduced a solution of fetuin (ca. 10 mg mL^{-1})—a glycosylated protein bearing oligosaccharides that terminate in NeuAc—into the sample suspension. The connections between cells and spheres dissociated over

  1433-7851/00/3919-3504 $ 17.50+.50/0

periods of about 45 min to 2 h, and the arrays disassembled. We believe this disassembly reflects competition of the sugar groups on fetuin with oligosaccharides on the cell surface for binding sites of WGA on the microspheres. The use of biospecific interactions to assemble these structures, and the consequent ability to disassemble them through competing interactions, distinguishes this method of fabrication with optical tweezers from methods that have used optical tweezers to align microspheres or colloids in 2D arrays and have frozen the resulting structures by photopolymerizing the solution that surrounded the particles.[16, 17]

Structures 2d and 2f are held together by nonbiospecific interactions. In these assemblies, we used unmodified polystyrene microspheres, which also adhere to the surface of erythrocytes. We connected the cells toghether by first attaching a sphere to each cell and then bringing the two spheres together. In contrast to the WGA-linked microspheres, the bare polystyrene spheres adhere to one another. The soluble carbohydrates that inhibited adhesion of WGA-linked spheres to erythrocytes did not block adhesion of bare polystyrene spheres. Suspending the polystyrene sphere in a solution of bovine serum albumin (BSA, 1 mg mL^{-1}) prior to bringing it into contact with the cell or with another sphere did prevent adhesion. These observations are consistent with the idea that adhesion with unmodified polystyrene spheres results from nonspecific (probably hydrophobic) interactions.

Figure 3 shows a microstructure built with two types of cells—erythrocytes and lymphocytes—connected by WGA-coated microspheres. Erythrocytes are characterized by their

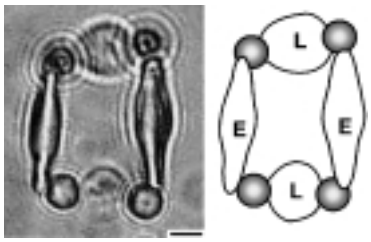

Figure 3. Optical micrograph and explanatory illustration of a composite structure with two cell types: erythrocytes and lymphocytes. The cells are connected by biospecific interactions between WGA-linked microspheres (gray spheres) and sugars on the surfaces of the cells. The erythrocytes are oriented perpendicularly to the cells in Figure 2. The bar in the micrograph represents 3 μm.

disk shape and by the rigidity and elasticity of their membranes; lymphocytes are globular, and their membranes tend to deform more easily.[18] In this structure, the erythrocytes were rotated by 90° with respect to the cells pictured in Figure 2, so their narrow edge is directed into the line of sight. We believe that the ability to incorporate several different cell types into one structure will be important in assays that require interactions among cells mediated by diffusable signaling molecules, and that address differences in response of different cell types to drugs, toxins, and environmental factors.

Fabrication of 3D microstructures is difficult. Optical tweezers should make it possible to assemble a range of structures. We illustrate this capability by the assembly of two 3D arrays of erythrocytes (Figure 4). The procedure for 3D

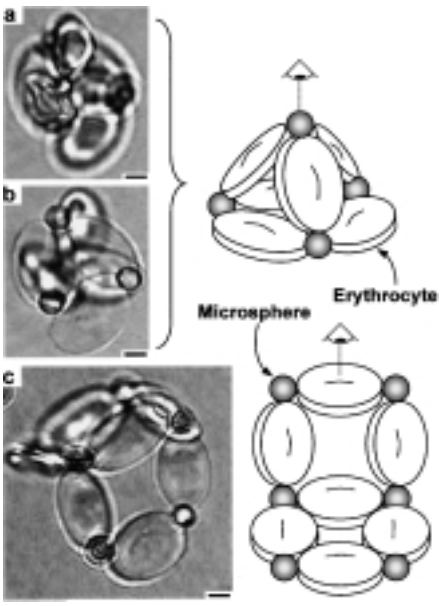

Figure 4. Optical micrographs and schematic illustrations of 3D arrays of erythrocytes. The micrographs in a) and b) are of the same tetrahedron imaged at two different focal planes: the image in a) was recorded with the focal plane near the apex of the assembly and the image in b) was recorded with the focal plan near the base of the assembly. In a) the apical microsphere is roughly in focus and in b) the cells and microspheres that make up the base are roughly in focus. The image in c) is that of two square planes joined perpendicularly along one edge. In the schematic drawings, the eye and the dotted line establish the line-of-sight used in generating the micrographs. The bar in each image represents 3 μm.

fabrication is analogous to that described for 2D structures.

The 3D microassembly by using light tweezers is, of course, not limited to biological components.[19–23] The application of optical tweezers in the fabrication of 2D and 3D structures should be generalizable to the assembly of a wide variety of objects with dimensions that range in size from μm to a few hundred nm; the practical size limitation is set by the size of the focal region of the laser beam, approximately $\lambda/2\pi$ (where λ is the wavelength of the light) or about 150 nm at the wavelength we have used.[24] The principal restrictions to the process are that the objects must have an index of refraction greater than that of the surrounding medium and that they must be transparent to the wavelength of the optical beam.[24] In addition, a wide variety of recognition systems can be exploited for attachment: examples include protein–ligand interactions,[4–6, 9] interactions between complementary strands of DNA,[25–27] capillary forces,[28] electrostatic forces,[3] and hydrophobic interactions.[2] The scope of the different shapes that can be exploited in fabrication has not been established. Optical tweezers have been employed to trap a variety of spherical and nonspherical objects, although theory that describes trapping nonspherical objects is not well established.[29, 30] A limitation of the procedure that we have described is that it is a serial method. We believe that the application of acousto-optic devices to generate arrays of optical traps from a single laser beam is one strategy that offers the potential to extend light-driven microfabrication into a parallel method.[16]

  1433-7851/00/3919-3505 $ 17.50+.50/0

The 2D and 3D structures shown in Figures 2–4 would be difficult to fabricate by other methods. The ability both to position and to orient nonspherical objects in 3D by using multiple light beams is a valuable characteristic of optical tweezers. We believe that light-driven microfabrication is an adaptable method that provides a broadly applicable solution to the problem of assembling micron-sized, optically transparent components into structured arrays. Its use with biological cells illustrates its capability in manipulating both nonspherical and fragile components.

Experimental Section

To prepare WGA-linked microspheres, spheres presenting primary amino groups (0.001 g mL^{-1}; polysciences) were suspended in a phosphate-buffered solution (ca. pH 6) of a dicarboxylic acid linker (HO_2C-$(CH_2CH_2O)_nCO_2H$; $n = 7-14$; 0.05 g mL^{-1}; Fluka), 1-[3-(dimethylamino)-propyl]-3-ethylcarbodiimide hydrochloride (EDC; 0.4 M), and *N*-hydroxy succinimide (NHS; 0.1 M). The suspension was agitated gently at room temperature for 8 h to couple the linker to the sphere. The beads were separated from the solution of reactants by centrifugation and resuspended in deionized water. This procedure was repeated three times. The beads were resuspended in a solution of EDC (0.4 M) and NHS (0.1 M) and agitated gently for 15 min. The beads were isolated by centrifugation and resuspended in a solution of WGA (0.5 mg mL^{-1}) in phosphate buffer (0.1 M, pH 8.1); the suspension was agitated gently for 4 h to couple WGA to active esters on the beads. The beads were isolated from the solution of WGA and stored in phosphate buffered saline.

The glass cover slips used to support the sample suspension were treated with tridecafluoro-1,1,2,2-tetrahydrooctyl-1-methyldichlorosilane (United Chemical Technologies) under vacuum for 3 h and then soaked the silanized slide in a solution of BSA (0.05 g mL^{-1}). This procedure introduced a monolayer of BSA that blocks nonspecific adsorption to the glass.

We used three optical traps (optical tweezers) that could be manipulated independently. One trap was created by using a collimated beam from a Helium-Neon (HeNe) laser (power = 22 mW). The beam was expanded in stages by two telescopes; a steering mirror was placed between these telescopes to allow us to adjust the position of the optical trap within the sample. A high power (100×, numerical aperture = 1.2) oil immersion microscope objective focused the beam into the sample. A lens placed before the objective converted the collimated telescope output into a beam with the appropriate size and curvature. A dichroic mirror that transmits most visible light but reflects the light produced by the HeNe laser (632 nm) was used to direct the beam into the objective while allowing us to image the sample with a CCD video camera. The remaining two traps were generated by two linearly polarized diode lasers (852 nm) whose powers could be adjusted from 0 to about 100 mW. Each beam was collimated and passed through an anamorphic prism so that they were both roughly circular. Telescopes expanded each beam as necessary. We placed mirrors before each telescope to be used to steer the beams. The polarization of each beam was adjusted so the beams could be passed through a polarizing beam splitter. The resulting output was directed through a lens to adjust the radius of curvature and the size of the beams, then directed through a dichroic mirror to adjust the wavelength of the beams, and finally directed through the microscope objective and into the sample. This arrangement produced three optical traps within the sample. We used the near-infrared (852 nm) beams to trap the cells and the visible (632 nm) beam to trap the polystyrene microspheres.

Received: May 2, 2000 [Z15062]

[1] T. L. Steck, *J. Cell Biol.* **1974**, *62*, 1–19.
[2] G. M. Whitesides, E. E. Simanek, J. P. Mathias, C. T. Seto, D. N. Chin, M. Mammen, D. M. Gordon, *Acc. Chem. Res.* **1995**, *28*, 37–44.
[3] J. Tien, A. Terfort, G. M. Whitesides, *Langmuir* **1997**, *13*, 5349–5355.
[4] H. Lis, N. Sharon, *Chem. Rev.* **1998**, *98*, 637–674.
[5] *Extracellular Matrix* (Eds.: M. A. Zern, L. M. Reid), Marcel Dekker, New York, **1993**.
[6] T. Feizi, P. R. Crocker, *Curr. Opin. Struct. Biol.* **1996**, *6*, 679–691.
[7] Y. Nagata, M. M. Burger, *J. Biol. Chem.* **1974**, *249*, 3116–3122.
[8] B. P. Peters, S. Ebisu, I. J. Goldstein, M. Flashner, *Biochemistry* **1979**, *18*, 5505–5511.
[9] C. S. Chen, M. Mrksich, S. Huang, G. M. Whitesides, D. E. Ingber, *Science* **1997**, *276*, 1425–1428.
[10] A. Ashkin, J. M. Dziedzic, J. E. Bjorkholm, S. Chu, *Opt. Lett.* **1986**, *11*, 288–291.
[11] M. Mammen, K. Helmerson, R. Kishore, S. K. Choi, W. D. Phillips, G. M. Whitesides, *Chem. Biol.* **1996**, *3*, 757–763.
[12] F. Jordan, E. Bassett, W. R. Redwood, *Biochem. Biophys. Res. Commun.* **1977**, *4*, 1015–1021.
[13] M. Mammen, S. K. Choi, G. M. Whitesides, *Angew. Chem.* **1998**, *110*, 2908–2953; *Angew. Chem. Int. Ed.* **1998**, *37*, 2755–2794.
[14] J. Rao, J. Lahiri, L. Isaacs, R. M. Weis, G. M. Whitesides, *Science* **1998**, *280*, 708–711.
[15] J. Rao, J. Lahiri, R. M. Weis, G. M. Whitesides, *J. Am. Chem. Soc.* **2000**, *122*, 2968–2710.
[16] D. W. M. Marr, C. Mio, *Langmuir* **1999**, *15*, 8565–8568.
[17] H. Misawa, K. Sasaki, M. Koshioka, N. Kitamura, H. Masuhara, *Appl. Phys. Lett.* **1992**, *60*, 310–312.
[18] *Hematology* (Eds.: W. J. Williams, E. Beutler, A. J. Erslev, R. W. Rundles), McGraw Hill, New York, **1972**.
[19] E. R. Dufresne, D. G. Grier, *Rev. Sci. Instrum.* **1998**, *69*, 1974–1977.
[20] A. Ashkin, J. M. Dziedzic, T. Yamane, *Nature* **1987**, *330*, 769–771.
[21] A. Ashkin, J. M. Dziedzic, *Science* **1987**, *235*, 1517–1520.
[22] K. Svoboda, S. M. Block, *Ann. Rev. Biophys. Biomol. Struct.* **1994**, *23*, 247–285.
[23] K. Svoboda, S. M. Block, *Opt. Lett.* **1994**, *19*, 930–932.
[24] S. P. Smith, S. R. Bhalotra, A. L. Brody, B. L. Brown, E. K. Boyda, M. Prentiss, *Am. J. Phys.* **1999**, *67*, 26–35.
[25] C. A. Mirkin, R. L. Letsinger, R. C. Mucic, J. J. Storhoff, *Nature* **1996**, *382*, 607–609.
[26] G. P. Mitchell, C. A. Mirkin, R. L. Letsinger, *J. Am. Chem. Soc.* **1999**, *121*, 8122–8123.
[27] C. J. Loweth, W. B. Caldwell, X. G. Peng, A. P. Alivisatos, P. G. Schultz, *Angew. Chem.* **1999**, *111*, 1925–1929; *Angew. Chem. Int. Ed.* **1999**, *38*, 1808–1812.
[28] N. Bowden, I. S. Choi, B. A. Grzybowski, G. M. Whitesides, *J. Am. Chem. Soc.* **1999** *121*, 5373–5391.
[29] A. L. Stout, W. W. Webb, *Meth. Cell Biol.* **1998**, *55*, 99–116.
[30] A. Rosin, T. Wohland, E. Stelzer, *Zool. Stud.* **1995**, *34*, 167–169.

  1433-7851/00/3919-3506 $ 17.50+.50/0